



ELSEVIER

Journal of Chromatography A, 859 (1999) 13–21

JOURNAL OF  
CHROMATOGRAPHY A

www.elsevier.com/locate/chroma

# Time-resolved high-performance liquid chromatography fluorescence detector using a nanosecond pulsed light source for detecting lanthanide-chelated compounds

Tetsuo Iwata<sup>a,\*</sup>, Jun Koshoubu<sup>b</sup>, Yasuyuki Kurosu<sup>c</sup>, Tsutomu Araki<sup>d</sup>

<sup>a</sup>Department of Mechanical Engineering, Faculty of Engineering, University of Tokushima, Minami-Jyosanjima-2, Tokushima 770-8506 Japan

<sup>b</sup>JASCO Technical Research Laboratories Corporation, 2097-2, Ishikawa, Hachioji, Tokyo 192-0032 Japan

<sup>c</sup>The Department of Biochemistry, Juntendo University, School of Medicine, 2-1 Hongo, Bunkyo-ku, Tokyo 113-0033, Japan

<sup>d</sup>Department of Systems and Human Science, Graduate School of Engineering Science, Osaka University, Toyonaka, Osaka 560-8531 Japan

Received 18 February 1999; received in revised form 25 May 1999; accepted 21 July 1999

## Abstract

We have constructed a time-resolved fluorescence detection (TRFD) system for the analysis of amino compounds with high-performance liquid chromatography (HPLC) using lanthanide ion chelates. In order to carry out time-resolved measurements, we have employed a nanosecond pulsed xenon-arc lamp as an excitation light source. Amino compounds derivatized by isothiocyanobenzyl-EDTA (IEDTA) with the lanthanide chelate are mixed with an enhancer solution in a post-column manner and detected by TRFD. Taking advantage of a property of the long fluorescence lifetime of the lanthanide chelates, high selectivity against background fluorescence was achieved. In order to demonstrate the usefulness of TRFD, fundamental performance tests were carried out. Details of the system are also described. © 1999 Elsevier Science B.V. All rights reserved.

**Keywords:** Fluorescence detection; Detection, LC; Instrumentation; Lanthanides; Metal chelates

## 1. Introduction

Fluorescence properties of lanthanide ion chelates are characterized by large Stokes shift, a narrow band width of emission, high quantum yields, and long lifetimes ranging from tens of microseconds to submilliseconds [1–10]. By taking advantage of the high quantum yields or the resultant high fluorescence intensity, the lanthanide chelates have been

used as labels for immunological assays, instead of the conventional radioisotopes, for safety considerations [10,11]. On the one hand, by paying attention to the long fluorescence lifetimes, time resolved fluorometry has been proposed [9,12–14]. The aim of the time resolved fluorometry is to enhance the detection selectivity. This is performed in the time domain by separating the analyte fluorescence signal from the background fluorescence by using an pulsed excitation source. When we use a time gate with a suitable time delay after the pulsed excitation, we can easily discriminate between them. This is be-

\*Corresponding author. Fax: +81-88-656-9082.

E-mail address: iwata@me.tokushima-u.ac.jp (T. Iwata)

cause the fluorescence lifetimes of the background materials are short ( $<10^{-8}$  s), whereas those of lanthanide chelates are very long ( $>10^{-5}$  s).

If we use the time-resolved fluorometric technique in the field of high-performance liquid chromatography (HPLC) or capillary zone electrophoresis (CZE), more enhancement in separation selectivity is expected [12,15–19]. For instance, a highly overlapped chromatographic peak could be separated or isolated easily in the time domain spectroscopically, otherwise it cannot be resolved at all chromatographically due to the limitation of the choice of the buffer solution and/or to that of analysis time. Furthermore, in order to eliminate the light scattering of the excitation beam from the surface of the sample cell or to reject the background fluorescence signal from some kinds of contaminations, a simple, low-cost, filter spectroscopic method could be employed, otherwise the conventional grating monochromator must be used. Another advantage in using the filter spectrometric method is its high optical throughput over the grating monochromator. In addition, the large Stokes shift mentioned above suits the filter spectroscopic method. After all, the aim of the time-resolved technique in HPLC or CZE is not to improve the detection sensitivity (or detection limits) directly but to enhance the detection selectivity. The detection limits are improved only when the interfering background signal is dominant in practical analysis rather than in laboratory-level analysis.

Based upon such an idea, we constructed and reported a time-resolved fluorescence detection (TRFD) system for HPLC using europium chelates [20]. For the purpose of the time-resolved measurements, we used a combination of a dc-operated xenon lamp (75 W) and two mechanical choppers. The duty ratios and the rotational phase between the two choppers inserted in the excitation and emission sides were suitably controlled by a phase-locked-loop circuit. We employed such an optical configuration by taking into account the properties of the europium chelates: long lifetimes and high intensity. Although the TRFD system worked quite well for analysis of the europium chelated compounds, there was a problem when analyzing samarium or terbium chelates whose fluorescence lifetimes were less than 100  $\mu$ s. This was because the separation between the excitation light and the fluorescence decay signals

became difficult due to the instrumental function, that was, the relatively large duration of the excitation pulse (75  $\mu$ s) introduced by the mechanical choppers. In order to make the TRFD system more commonly useful, therefore, a light source whose pulse duration is sufficiently narrow is required. Although the commercially available flash xenon lamp, for example L4318 (Hamamatsu Photonics), offers us an intense light pulse with a pulse duration of a few microseconds, it has some problems in the signal-to-noise ratio ( $S/N$ ) in actual analysis because of a relatively low repetition frequency ( $<100$  Hz; usually 10 Hz) and of large inductive noise.

We, therefore, have newly constructed a time-resolved HPLC fluorescence detector by using a nanosecond, pulsed xenon-arc lamp that had been developed by one of authors [21]. The characteristics of the pulsed xenon lamp are as follows: (1) sufficiently narrow pulsewidth [full width at half-maximum (FWHM),  $t_w=3.0$  ns], (2) high repetition frequency ( $f>1$  kHz) depending on the applied voltage, (3) broad band spectrum ranging from 250 to 650 nm, (4) high intensity (peak power,  $P>20$  W), (5) low cost and simple to construct. The relative emission intensity in the ultraviolet region over the visible one is enhanced in comparison with that of the conventional dc-operated xenon lamp because of the high electron temperature (see fig. 5 in Ref. [21]). By using the stable, high intensity, high repetition frequency, nanosecond lamp, the optical system became compact and simple in comparison with the previous one. Furthermore, the new system has the possibility in the future for detecting many kinds of fluorescent compounds derivatized (or not derivatized at all) by other reagents except lanthanide ions, whose fluorescence lifetimes are in a nanosecond region. In the present article, we describe the instrument in detail and show new experimental results.

## 2. Instrumentation

### 2.1. Pulsed light source

Fig. 1 shows a photograph of the pulsed xenon lamp and its equivalent circuit. Different points between the previously constructed lamp and this

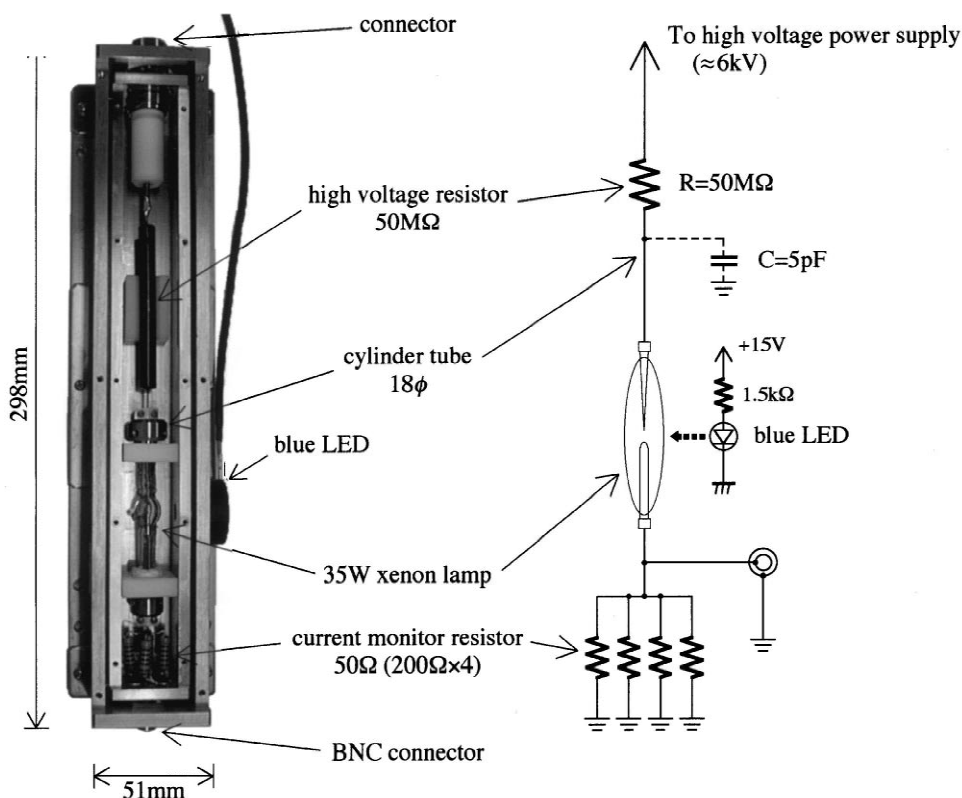


Fig. 1. A photograph of a xenon discharge lamp and its equivalent circuit diagram.

one are as follows: (1) The lamp is housed in a double rectangular brass box (inner width: 25 mm; inner height: 25 mm; inner length: 270 mm; thickness: 5.0 mm) instead of the conventional cylinder case by taking account of easiness of construction and that of maintenance. (2) In order to make a time base pulse for synchronization, we put a current monitor resistor ( $r=50\ \Omega$ ): A voltage pulse signal induced by discharge current across the resistor is picked up. This alternation is based on a fact that the time jitter (less than 10 ns) in sampling operation is negligible in comparison with the analyte lifetimes; which makes the system's configuration simple. (3) A blue-colored light emitting diode (LED; Model 520 in NLPB series, Nichia Chemical Industries, Japan) driven by 20 mA dc-current was attached beside the xenon lamp in order to lower the breakdown voltage of the lamp and to stabilize the pulsing operation. In a dark place, the breakdown voltage was 5.5 kV with the LED, whereas more than 9 kV

was required without the LED. Time jitter in the repetitive emission was also reduced markedly by using the LED. The blue light from the LED seems quite useful for preionizing the inserted gas in the lamp or for lowering the work function of the metal electrode in the lamp. We are now studying this phenomenon.

A lamp used was a xenon arc lamp (35 W type; L2173, Hamamatsu Photonics) whose electrode gap distance was 1.0 mm. The lamp has two electrodes, one with a sharpened end and the other with a round end. We used the sharpened end electrode as an anode and the round one as a cathode, the connections of which were reversed against those of the normal dc operation mode. This is because the reverse connection gives a stable, smooth, and intense pulse emission [21]. The anode electrode is connected to the positive power supply (10 kV, 3 mA; HJL-10P3, Matsusada Precision, Japan) through a high voltage resistor R (GS3-50MW, Tama Elec-

tric, Japan), while the cathode electrode is connected to ground through the monitor resistor ( $r=50\ \Omega$ ); where the resistor,  $r$ , consists of four  $200\ \Omega$  ( $1\ \text{W}$ ) resistors connected in parallel. A capacitor shown as C is formed between a brass cylinder (18 mm in diameter) attached on the anode electrode and the lamp enclosure. The capacitance value was estimated to be about 5 pF. The capacitance is charged through R from the high-voltage power supply until voltage between the electrodes reaches the breakdown voltage of the electrode gap. The charged electrons on the capacitor start flowing through the gap immediately after breakdown, thereby generating a short and intense discharge plasma between the gap. The charge–discharge process occurs successively, resulting in the production of repetitive and fast light pulses. From performance tests, we obtained the

following specifications:  $t_w=3.0\ \text{ns}$ ,  $f\approx 1\ \text{kHz}$ , and  $P=100\ \text{W}$  under the applied voltage of  $V=6.2\ \text{kV}$ .

## 2.2. Time-resolved fluorescence detector

### 2.2.1. Optical system

Fig. 2 shows the optical system of TRFD for HPLC. A light flux emitted from the pulsed lamp is focused onto the center of the HPLC cell through a UV band-pass filter (F1; UTVAF-50S-34U, Sigma Koki). The transmission wavelength of the filter was between 280 and 370 nm (at  $-3\ \text{dB}$  points) with a maximum at 340 nm. The fluorescence emitted from the analyte in the cell is focused on a cathode of a metal-packaged, compact, photomultiplier tube (PMT; H5783-01, Hamamatsu Photonics) through a low-pass optical filter (F2; SCF-50S-54O),  $-3\ \text{dB}$

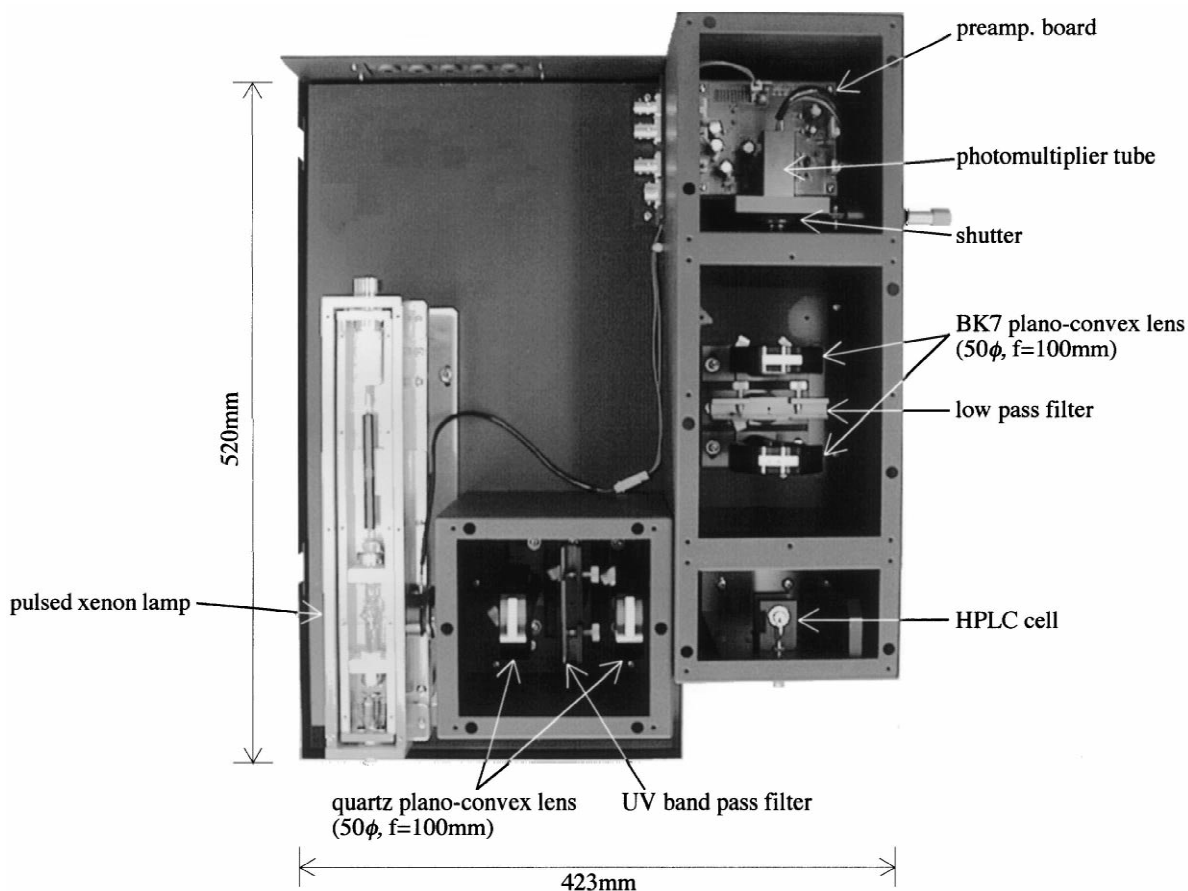


Fig. 2. Optical system of the time-resolved fluorescence detector for HPLC (top view).

wavelength of which is 540 nm. The wavelength characteristics of the two filters are suitable for measuring fluorescence signals of lanthanide chelates. The optical system is very simple. This is because: (1) the filter spectroscopic method can be employed by taking account of the large Stokes shift of the fluorescence properties of the lanthanide chelates, (2) the intense, nanosecond pulsed light source is employed.

### 2.2.2. Signal processing circuit

A circuitry block diagram of signal processing circuit after the PMT is shown in Fig. 3. It consists of an analog part and a digital part. In order to obtain relatively large voltage signals at the cost of time resolution, the value of the load resistor for the PMT was set to be  $R_1=500 \text{ k}\Omega$ . Although the time constant of the input integration circuit was found to be about 5 ms, there was no problem in the time-resolved measurements because of the long fluorescence lifetimes of the lanthanide chelates. After passing through a preamplifier (PA) and an offset compensation circuit (OC), the voltage signal is fed into a gated-type integrator circuit that consists of an analog switch (AS) and an RC filter ( $R_2$  and  $C_2$ ; time constant,  $\tau=10 \text{ ms}$ ). The output from the gated-type integrator is finally fed into a chart recorder through a sample and hold (S/H) circuit, an amplifier (A), and a buffer amplifier (BA).

The digital part generates timing signals for the analog circuit by using three monostable multivibrators (MS). The timing diagram is shown in Fig. 4. In order to eliminate the unfavorable background fluorescence signal, which is schematically shown in Fig. 4b by a dashed line, a gate pulse (Fig. 4d) for the gated-type integrator is delayed by  $T_d$  (Fig. 4c) from the time base signal (Fig. 4a). The accumulated fluorescence signal due to the lanthanide chelates is depicted in Fig. 4b by hatched lines. Normal operating conditions are as follows:  $f=1.0 \text{ kHz}$  (period  $T=1.0 \text{ ms}$ ), gate pulsewidth  $T_{\text{gw}}=100 \text{ }\mu\text{s}$ . The value of the observed time constant of the gated-type integrator, therefore, becomes  $t_{\text{obs}} = \tau T / T_{\text{gw}} = 100 \text{ ms}$ , the value of which is suitable for HPLC analysis. The value of the time delay,  $T_d$ , is optimized experimentally. Fig. 4e shows a timing signal for the S/H circuit. In order to prevent malfunction due to high frequency operation of the pulsed lamp, an

inhibiting signal (Fig. 4f) is fed into the input part of the digital circuit. The signal processing circuit is very simple as well as the optical system. This is again thanks to the fluorescence properties of the lanthanide chelates: long lifetimes and high intensity.

## 2.3. HPLC system

### 2.3.1. Flow system

An HPLC flow system consists of the following components: pump #1 and pump #2 (plunger type PU-980, JASCO), a six-way sample injector (Rheodyne 7175; 20  $\mu\text{l}$  loop), a mixing coil (Tefzel, 4 m $\times$ 0.25 I.D.), and the TRFD system. Pump #1 is used for delivery of the eluent, and pump #2 for delivering post-column reagent (enhancer solution). The analyte solution injected was passed through a separation column, together with the eluents. Individual components of the analyte solution separated by the column are mixed with the enhancer solution from pump #2 and then lanthanide ion chelates were reformed. Finally, the lanthanide chelates pass through the HPLC flow-cell and are detected by TRFD. The mixing coil inserted between the column and the cell was immersed in a temperature controlled water bath at 40°C in order to promote the reaction. The volume in the flow cell used for TRFD was 16  $\mu\text{l}$ . The mobile phase was 20 mM sodium phosphate (pH 6.0) containing 10% acetonitrile at a flow-rate of 0.1 ml/min. The post-column reagent used was pivaloyltrifluoroacetone (PTA) or thenoyltrifluoroacetone (TTA) solution, at a flow-rate of 0.04 ml/min. A 50 $\times$ 0.15 mm I.D. stainless steel column packed with Crest C1-5 (JASCO) or Develosil TMS-UG-5 (Nomura) was used.

### 2.3.2. Chemicals

For HPLC, a sample solution derivatized by isothiocyanobenzyl-EDTA (IEDTA) and/or maleimido-C5-benzyl-EDTA (MEDTA) with a lanthanide ion chelate is mixed with an enhancer solution in a post-column manner. The enhancer solution consists of a  $\beta$ -diketone, tri-*n*-octylphosphine oxide (TOPO), and a surfactant (TritonX-100). The  $\beta$ -diketone used was either PTA or TTA. TritonX-100 and europium acetate were purchased from Wako (Osaka, Japan), and PTA, TTA, TOPO,

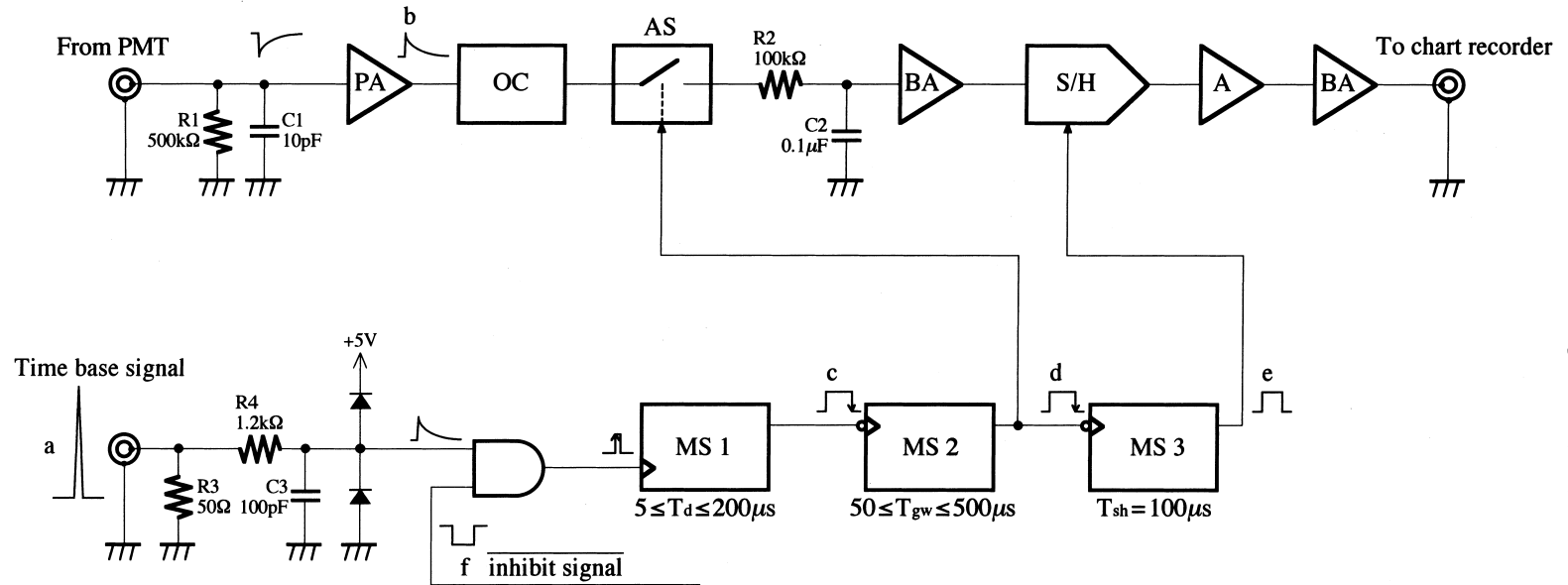


Fig. 3. Circuitry block diagram of the signal processing in the TRFD system. PA; preamplifier, OC; offset compensation, AS; analog switch, S/H; sample and hold, BA; buffer amplifier, A; amplifier, MS; monostable multivibrator.

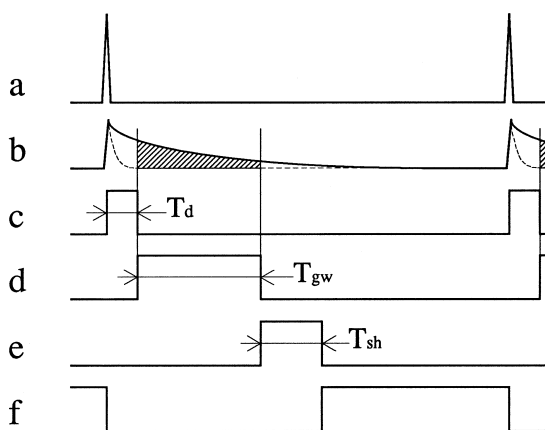


Fig. 4. Timing diagram of the signal processing circuit: (a) time base signal obtained from the pulsed lamp, (b) fluorescence signals due to lanthanide chelates (solid line) and to background (dashed line), (c) delay pulse generated by MS1, (d) gate pulse generated by MS2, (e) S/H pulse generated by MS3, (f) inhibit signal.

IEDTA and MEDTA from Dojin (Kumamoto, Japan). All other reagents were of analytical grade.

### 2.3.3. Preparation of the enhancer solution

To 5 g of Triton X-100 in distilled water (100 ml), 50 ml of 2 M sodium acetate (pH 6.5), 5 ml of 50 mM TOPO (acetonitrile solution), and 16 ml of 2.5 mM  $\beta$ -diketone (acetonitrile solution) were added. The solution was diluted to 500 ml with distilled water. Final concentration of Triton X-100, sodium acetate, TOPO and  $\beta$ -diketone were 1.0%, 200 mM, 500  $\mu$ M, and 80  $\mu$ M, respectively.

### 2.3.4. Derivatization of amino compounds

To 1  $\mu$ M~1 mM amine solution (10  $\mu$ l), 5~500  $\mu$ M lanthanide (Ln; Ln=Eu or Sm) chelate of IEDTA (IEDTA–Ln; 45  $\mu$ l), and 100 mM sodium carbonate (pH 9.0; 45  $\mu$ l) were added. The mixture was incubated for 4 h at 40°C, and 5  $\mu$ l of the reaction mixture was introduced into the HPLC column. The IEDTA–Ln solution was prepared by addition of IEDTA (1 mg) to 0.5 mM lanthanide acetate solution.

### 2.3.5. Derivatization of thiol compounds

This derivatization was usually carried out after derivatization for amines. To 1  $\mu$ M~1 mM thiols (10

$\mu$ l), 5~500  $\mu$ M lanthanide (Ln) chelate of MEDTA (MEDTA–Ln; 45  $\mu$ l), and 100 mM sodium carbonate (pH 9.0~9.8; 45  $\mu$ l) were added. After incubation for 5 min at room temperature, 10  $\mu$ l of 1 M Bis-Tris (pH 9.5) was added and then 5  $\mu$ l of the reaction mixture was introduced into the HPLC column. The MEDTA–Ln solution was prepared by addition of MEDTA (1 mg) to 0.5 mM lanthanide acetate solution.

### 2.3.6. Sample preparation of tainted fish meat

The fish meat was stored at room temperature for a week for decomposition. The tainted fish meat was homogenized in a mixer in two volumes of distilled water. The homogenate was centrifuged at 10 000g for 30 min. The precipitate and suspended matter were removed. To the supernatant, the same volume of ethanol was added and stirred at room temperature for 5 min. After standing at room temperature for 1 h, it was centrifuged at 10 000 g for 30 min. The supernatant was used as a mixture including amine and thiol compounds.

## 3. Results and discussion

First, we have checked the background rejection capability of TRFD in the same way as before [20]. We operated TRFD in a flow injection analysis (FIA) mode (that is, HPLC system without a separation column) in the presence of a strongly interfering fluorescent background. This was because the HPLC column had a slight memory effect for the lanthanide chelated compounds which prevented the accurate evaluation of the performance of the TRFD system itself. The background material was various concentrations (100–900  $\mu$ M) of Fluorecein whose lifetime was a few nanoseconds. In such a situation, we were able to discriminate fluorescence between 0.1  $\mu$ M Eu<sup>3+</sup> chelate sample and the background Fluorecein. The capability for eliminating the background fluorescence was examined in another experiment by using 1 ppm quinine sulfate in 0.05 M H<sub>2</sub>SO<sub>4</sub> (whose lifetime is less than 20 ns) and found to be good as before [20].

In order to demonstrate the overall performance of TRFD for HPLC, we have analyzed a mixed solution of 66.7 mM 3-phenyl-1-propylamine-IEDTA-Eu (P-

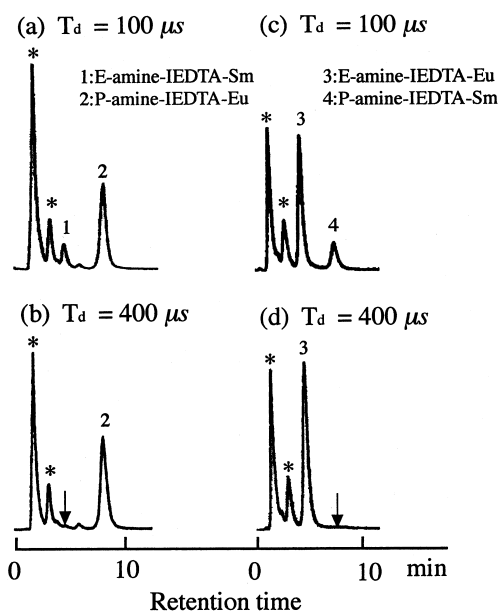


Fig. 5. (a) Chromatogram of a mixed solution of  $66.7 \mu M$  3-phenyl-1-propylamine-IEDTA-Eu (P-amine-IEDTA-Eu) and  $66.7 \mu M$   $\beta$ -phenethyl amine-IEDTA-Sm (E-amine-IEDTA-Sm) obtained with  $T_d = 100 \mu s$  and  $T_{gw} = 100 \mu s$ , (b) that obtained with  $T_d = 400 \mu s$  and  $T_{gw} = 100 \mu s$ , (c) chromatogram of a mixed solution of  $66.7 \mu M$  P-amine-IEDTA-Sm and  $66.7 \mu M$  E-amine-IEDTA-Eu obtained with  $T_d = 100 \mu s$  and  $T_{gw} = 100 \mu s$ , (d) that obtained with  $T_d = 400 \mu s$  and  $T_{gw} = 100 \mu s$ . Peaks marked \* represent by-products of the IEDTA reaction.

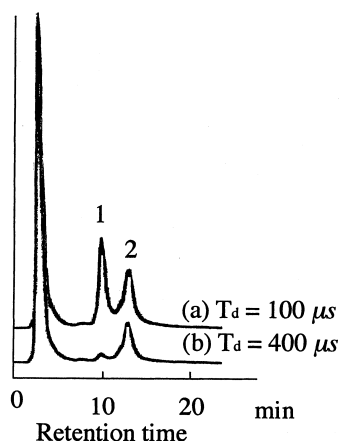


Fig. 6. (a) Chromatogram of a mixture including amine and thiol compounds from tainted fish meat obtained with  $T_d = 100 \mu s$  and  $T_{gw} = 100 \mu s$ , (b) that obtained with  $T_d = 400 \mu s$  and  $T_{gw} = 100 \mu s$ . Peak tentative assignment: 1, thiol component; 2, amine component. Sample was derivatized by IEDTA-Eu for amines and then by MEDTA-Sm for thiols.

amine-IEDTA-Eu) and  $66.7 \text{ mM}$   $\beta$ -phenethyl amine-IEDTA-Sm (E-amine-IEDTA-Sm) with the Crest C1-5 column. A chromatogram obtained from the TRFD is shown in Fig. 5a, where  $T_d$  and  $T_{gw}$  were both  $100 \mu s$ . On the one hand, Fig. 5b shows a chromatogram obtained with  $T_d = 400 \mu s$  and  $T_{gw} = 100 \mu s$ . The E-amine-IEDTA-Sm peak had disappeared (shown by an arrow) because of its short lifetime ( $< 100 \mu s$ ) in comparison with that of P-amine-IEDTA-Eu ( $> 500 \mu s$ ). The peak marked \* were due to by-products of the IEDTA reaction. Figs. 5c and d shows the same experimental results but for the mixed solution of P-amine-IEDTA-Sm and E-amine-IEDTA-Eu. These results again show the selectivity of TRFD.

Fig. 6 shows chromatograms of the mixture including amine and thiol compounds from the tainted fish meat. Fig. 6a shows a chromatogram obtained with  $T_d = 100 \mu s$  ( $T_{gw} = 100 \mu s$ ) and Fig. 6b with  $T_d = 400 \mu s$  ( $T_{gw} = 100 \mu s$ ). The separation column used was Develosil TMS-UG-5. A peak tentatively assigned 1 is due to the thiol component derivatized by MEDTA-Sm. That assigned 2 is due to the amine components derivatized by IEDTA-Eu. These results show that the two kinds of components were discriminated with respect to each other by TRFD in HPLC analysis.

Next, TRFD was operated in a stopped-flow-analysis mode again in order to examine the detection limit. The sample solution used was europium acetate, samarium acetate, or terbium acetate dissolved in the enhancer solution (0.1% Triton X-100, 20 mM sodium acetate, 50  $\mu M$  TOPO, 8  $\mu M$  PTA; pH 6.5). The values of  $T_d$  and  $T_{gw}$  were both fixed at  $100 \mu s$ . For europium acetate, the detection limit was found to be  $5.0 \cdot 10^{-10} \text{ M}$  ( $7.9 \cdot 10^{-15} \text{ mol}$ ), for terbium acetate,  $4.2 \cdot 10^{-9} \text{ M}$  ( $6.5 \cdot 10^{-14} \text{ mol}$ ), and for samarium acetate,  $9.0 \cdot 10^{-9} \text{ M}$  ( $1.4 \cdot 10^{-13} \text{ mol}$ ). Here, we defined the detection limit as a sample concentration that gave  $S/N = 3$ .

The results of the detection limits in the present detection system were not so more improved in comparison with those in the previous version [20], and were somewhat far from real trace-level detection in a pure laboratory. We, however, should bear in mind again that the aim of TRFD is to enhance the detection selectivity rather than to improve the detection limits, as described in the



Introduction section. Indeed, TRFD has a lower signal gathering efficiency by the duty ratio, in principle, than the standard dc-operated detector. However, TRFD is useful for eliminating a high background or for isolating overlapped chromatographic peaks. The results shown in Figs. 5 and 6 should be understood from such a view point, that is, demonstrating the fundamental performance of TRFD for model samples. A decrease in the duty ratio in the present system than that in the previous one was covered by the higher intensity of the new lamp. In addition, unlike the previous system, the present one has a possibility for detecting nanosecond-fluorescence-lifetime compounds directly without using lanthanide chelates by making a slight modification in detector electronics. The appearance of by-product peaks in Fig. 5 deteriorates the detection selectivity as well as the detection limits and its elimination is an important problem for future study.

## References

- [1] Y. Okabayashi, T. Kitagawa, *Anal. Chem.* 66 (1994) 1448.
- [2] M. Schreurs, G.W. Somsen, C. Gooijer, N.H. Velthorst, R.W. Frei, *J. Chromatogr.* 482 (1989) 351.
- [3] T.J. Wenzel, L.M. Collette, D.T. Dahlen, S.M. Hendrickson, L.W. Yarmaloff, *J. Chromatogr.* 433 (1988) 149.
- [4] Y. Ci, Y. Li, X. Liu, *Anal. Chem.* 67 (1995) 1785.
- [5] T. Taketatsu, *Talanta* 29 (1982) 397.
- [6] M. Aihara, M. Arai, T. Taketatsu, *Analyst* 111 (1986) 641.
- [7] A.L. Jenkins, G.M. Murray, *Anal. Chem.* 68 (1994) 2974.
- [8] T.J. Wenzel, K. Zomlefer, S.B. Rapkin, R. Hkeith, *J. Liq. Chromatogr.* 18 (1995) 1473.
- [9] M. Schreurs, L. Hellendoorn, C. Gooijer, N.H. Velthorst, *J. Chromatogr.* 552 (1991) 625.
- [10] E. Soini, I. Hemmila, *Clin. Chem.* 25 (1979) 353.
- [11] J. Yuan, K. Matsumoto, H. Kimura, *Anal. Chem.* 70 (1998) 596.
- [12] S.D. Soper Jr., B.L. Legendre, D.C. Williams, *Anal. Chem.* 67 (1995) 4358.
- [13] A. Rieutord, L. Vazquez, M. Soursac, P. Prognon, J. Blais, Ph. Bourget, G. Mahuzier, *Anal. Chim. Acta* 290 (1994) 215.
- [14] B.I. Vazquez, C. Feute, C. Franco, A. Cepeda, P. Prognon, G. Mahuzier, *J. Chromatogr. A* 727 (1996) 185.
- [15] N. Furuta, A. Otuki, *Anal. Chem.* 55 (1983) 2407.
- [16] M. Latva, T. Ala-Kleme, H. Bjennes, J. Kankare, K. Haapakka, *Analyst* 120 (1995) 367.
- [17] K.J. Millrer, F.E. Lytle, *J. Chromatogr.* 648 (1993) 245.
- [18] B.L. Legendre Jr., S.A. Soper, *Appl. Spectrosc.* 50 (1996) 1196.
- [19] R.A. Baumann, C. Gooijer, Nel H. Velthorst, R.W. Frei, *Anal. Chem.* 57 (1985) 1815.
- [20] T. Iwata, M. Senda, K. Kurosu, T. Tsuji, M. Maeda, *Anal. Chem.* 69 (1997) 1861.
- [21] T. Araki, A. Yamada, T. Uchida, *Rev. Sci. Instrum.* 64 (1993) 1758.